An Adaptive Filter to Reduce SAR Speckles: A Case Study of Mapping Inundation Extent on the North Carolina Floodplain Using the JERS-1 SAR Data

Tao Zheng and Yong Wang Center for Geographic Information Science and Department of Geography East Carolina University

An adaptive filter was developed to reduce speckles and to preserve the boundaries (e.g., a flooded/nonflooded boundary) on a synthetic aperture radar (SAR) image, and hence to improve the accuracy on the inundation extent mapping using the SAR data. Based on the counts of pixels in each category within a moving kernel, the filter used different filtering approaches to reduce the speckles and retain the boundaries. As an example, the authors used the original, median-filtered, and adaptive-filtered Japanese Earth Resource Satellite – 1 (JERS-1) SAR data to map a flood extent on the North Carolina coastal floodplain, and to investigate the effectiveness of the adaptive filtering through a comparison study of the derived flood extents. Spatial correlation analysis and accuracy evaluation indicated that the adaptively filtered SAR data achieved higher accuracy on the inundation maps than either the median-filtered or the original SAR data.

Introduction

Floods are one of the major natural hazards that cost lives, cause damage to property, and disrupt social and economic activities. The ability to map the flood extent correctly can provide critical information for immediate flood relief activity, and pre- and postflood mitigation. It is possible to use optical and radar remote sensing data to map the flood extent because the water and non-water surfaces, such as soil and vegetation, have distinctive signatures in the data. Because the optical sensor lacks the ability to penetrate vegetation canopies, its usage in densely forested areas can be limited. On the other hand, synthetic aperture radar (SAR) data are able to penetrate the canopies (Richards, 1987), and have been widely used in the mapping of flood extent (e.g., Imhoff et al. 1987, Hess et al. 1995, Melack and Wang 1998, Bourgeau et al. 2001, Wang 2003).

When using the SAR data for inundation mapping in forested environments one should be cautious with two facts. First, due to the enhanced double bounced trunk-ground interactions when a forested area is flooded, a stronger radar return has been observed as compared to forested area where the ground is nonflooded. Second, because of the

coherent processes of data processing used to create the SAR data (e.g., Ulaby et al. 1982), there are speckles or abnormal bright or dark spots on the SAR data and the speckles are a severe problem for interpretability of SAR data (Ulaby et al. 1982). The speckles or bright spots may be mistakenly interpreted as flooded forests. To reduce or remove the speckles, various spatial filters (e.g., Lee 1981, Lee et al. 1991, Lee et al. 1997, Jensen 2000) in addition to the commonly used median filter have been devised based on the mechanisms that create the speckles. Lee et al. (1994) provided a detailed review of the speckle filtering of SAR data. For example, Wang (2003) utilized a 7x7 median filter to reduce the speckle in studying the seasonal change of inundation on the North Carolina coastal floodplains using the Japanese Earth Resource Satellite - 1 (JERS-1) SAR data (http:// www.eorc.nasda.go.jp/JERS-1). One problem with the median filter is that it can smear the flooded/ nonflooded boundaries in open areas or forested environments. The smearing effect results because the filter always outputs the median value within a moving filtering kernel and ignores the distribution of the pixel values within that kernel, even though

the distribution may consist of important information about the speckles and boundaries. To overcome the median filter's shortcoming on smearing the boundaries, an adaptive filter that utilizes the counts of pixels in each category within a kernel has been developed. The filter uses different approaches according to the counts in order to effectively reduce the speckles and retain the boundaries at the same time. Thus, the objectives of this study were to: 1) develop the adaptive filter, 2) apply the filter to the JERS-1 SAR data in mapping a flood extent on the North Carolina coastal floodplain, 3) evaluate the filter's effectiveness of the speckle removal and boundary retention through a comparison study of the derived flooded extents from the original, median-filtered, and adaptivefiltered SAR data, and finally 4) investigate the accuracy of the inundation maps.

Analysis

An adaptive filter

The adaptive filter is a spatial filter that moves a pixel at a time from left to right one line at a time. The output is a new value for each filtered pixel produced by analyzing the counts of pixels of each category within the kernel in the hope to reduce the speckle and retain the boundary. Because there are three categories (open water, flooded forest, and non-flooded area) involved, the pixels within a kernel (e.g., 3x3, 5x5, 7x7, etc.) can be in a homogenous situation of one category, a boundary situation of two different categories, or a mixed situation of all three categories. The adaptive filter can detect which situation the kernel is in by analyzing the counts of pixels that belong to each category within the kernel, and then use different methods to output new values accordingly.

Based on the classification algorithm to be described, the pixels within a moving kernel are classified into one of the three categories (the actual pixel value on the input image is not changed). The number of pixels in each category is counted and ranked from the most to the least. The category having the most number of the pixels is the first populous category, the category that includes the second most pixels the second populous category, and so on. It should be noted that when the kernel moves cross

the image the pixel values and distribution change. Thus, the first, second, and third populous categories vary. Three situations and adaptive methods are considered when output a filtered pixel value:

- a) If the first populous category includes at least 60% of pixels within the kernel, then the kernel is at the homogeneous case of the first populous category. The center pixel (to be adaptively filtered) is assigned to the first populous category and its pixel value is output as the average value of all the pixels belonging to the first populous category. Therefore, a speckle is reduced if the center pixel does not belong to the first populous category or the pixel is an outlier of the first category.
- b) If the first populous category includes less than 60% of the pixels within the kernel, but the first and second populous categories combined include at least 70% of the pixels, the kernel is considered in the boundary situation of the first and second populous categories. To retain the boundary (first and then to de-speckle), the center pixel should be assigned as the first or second populous category depending on the relationships between the original value of the center pixel and the two categories' backscatter coefficient ranges. Using the classification algorithms (§2.3), one can divide the entire range of backscatter coefficient into three regions (Figure 1). The rules to separate the water/ nonflooded area (W/NFA) and the nonflooded area/flooded forest (NFA/FF) are two dividing lines. There are three possible combinations of the first and second populous categories:
 - 1) The first and second populous categories are water and nonflooded area (not necessarily in that order). In this situation, if the center pixel's original value is less than the W/NFA dividing value, the center pixel will be assigned as water and its output value will be the average value of all the pixels that belong to the water category. Otherwise, the center pixel will be assigned as nonflooded area and its output value will be the average value of all the pixels of the nonflooded area category.
 - 2) The first or second populous category is nonflooded area or flooded forest. In this case,

if the center pixel's original value is less than the NFA/FF dividing value, the center pixel will be assigned as nonflooded area and its output value will be the average value of all the pixels of the nonflooded area category. Otherwise, the center pixel will be assigned as flooded forest and its output value will be the average value of all the pixels that belong to the flooded forest category.

3) The first and second populous categories are water and flooded forest (not necessarily in that order). In this situation, the distances from center pixel's original value to the W/NFA dividing value ($D_{\text{O-W/NFA}}$) and to the NFA/FF dividing value ($D_{\text{O-W/NFA}}$) will be compared (Fig. 1). If $D_{\text{O-W/NFA}}$ is less than $D_{\text{O-NFA/FF}}$, the center pixel will be assigned as water and its output value will be the average of all pixels of the water category. Otherwise, the center pixel will be assigned as flooded forest and its output value will be the average of all pixels of the flooded forest category.

c) If neither a) nor b) is true, the kernel will be in an area where all three categories are present. Then, the center pixel will output its original value as the new value. In this case, the original value is preserved; this approach should retain an edge.

It should be noted that in implementation, for a 3x3 kernel, 60% and 70% of a total of 9 pixels are 5 and 6 pixels, respectively. For a 5x5 kernel, the 60%

and 70% of 25 pixels are 15 and 18 pixels, respectively, and so on so forth.

Study area and datasets

The study area outlined is on the floodplain of the Tar/Pamlico River, North Carolina, covering part of Pitt County on the west and Beaufort County on the east (Fig. 2). As the Tar River expands into the sound, the river is called the Pamlico River. The study area is about 128 km². Based on the statewide landuse and land cover layer created by the North Carolina Center for Geographic Information and Analysis, there are fifteen landuse and land cover types. Bottomland forests/hardwood swamps and cultivated areas are dominant.

Two sets of data were used: the JERS-1 SAR data and USGS color infrared digital orthorectified quarter quadrangles (DOQQs). The SAR is an L-band (24 cm wavelength) HH (horizontally transmitted and horizontally received) sensor on board the JERS-1 satellite launched into space by the National Agency of Space and Development of Japan (NASDA) in 1992. The SAR has a 35° off nadir incidence angle, and its image has a 75 km swath width with a nominal 18 x 18 m ground spatial resolution. The SAR collected global radar images until October 1998 when ceased operation (http:// www.eorc.nasda.go.jp/JERS-1). Through a sponsored program by the NASDA to East Carolina University, the JESR-1 SAR data are available to this study. The

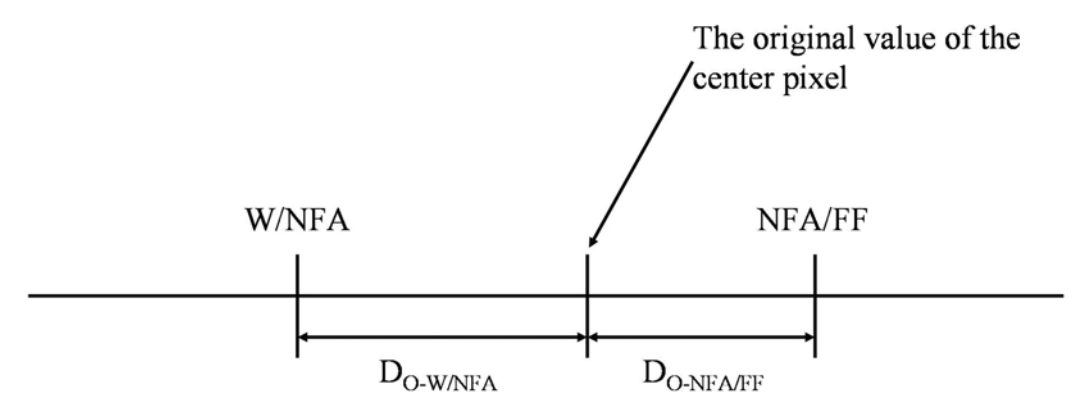


Figure 1. The distances from the original value of the center pixel to the water/nonflooded area (W/NFA) and nonflooded area/flooded forest (NFA/FF) dividing lines.

SAR data were acquired on 3 November 1994 and 10 June 1995, respectively. On the SAR images, the dark curve is the Tar River, which runs from the northwest corner to the southeast corner. The bright areas along the river banks are flooded forests, upland forests are in gray, and scattered patches of dark areas are flat surfaces, such as fields, bare soil, and pasture lands (Figure 2). The SAR images have been resampled to a 12.5 x 12.5 m resolution and absolutely calibrated by the NASDA. The conversion between a pixel intensity value (*I*) of the SAR image and backscatter coefficient ($^{\circ}$, in Decibel or *dB*) is:

The DOQQs created in 1998 are digital photographic data with a spatial resolution of 1 x 1 m. Due to its high resolution, water bodies, river channel, banks, upland forests, and some flooded forests can be easily identified. The DOQQ data in conjunction with limited ground observations are used to identify training and test sites for the water, nonflooded area, and flooded forest categories, so that the supervised classification algorithms for the SAR data can be used and their classification accuracy evaluated.

$$\sigma^0(dB) = 20.0 \times \log_{10} I - 85.34$$

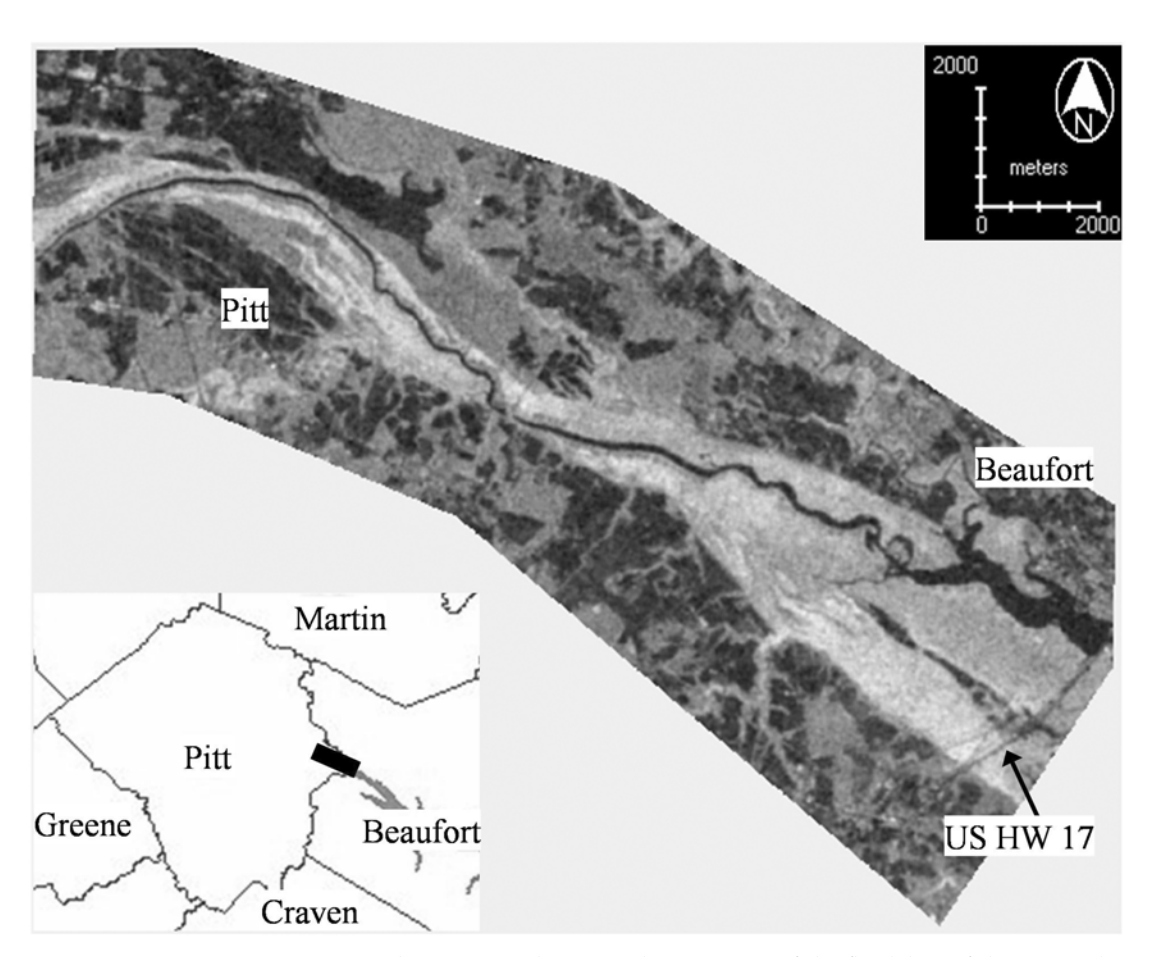


Figure 2. JERS-1 SAR image acquired on 3 November 1994 shows portion of the floodplain of the Tar/Pamlico River. The curved and dark signature is the river. The study area is about 128.0 km².

Analytical method

The analytical approaches enabled us to: 1) model inundation extents using the original, median-filtered, and adaptive-filtered SAR data, 2) compare the extents spatially, and 3) perform an accuracy assessment of the extents. To map the inundation extent, the SAR data were classified into three categories: open water, non-flooded area, and flooded forests based on the intensity of a pixels' backscatter coefficients. In general, the flat surfaces (such as an open water body) lead to a low backscatter coefficient. Flooded forest area has a high backscatter due to the double bounce interactions between a tree trunk and underneath water surface. The backscatter coefficient of non-flooded forest, crop fields, and pasture lands is in between.

To develop the classification algorithms, the SAR data were first filtered using a 5x5 median filter. Because of the temporal variation in inundation extents of the study area caused by the variation of river's discharge and flow condition, the training (as well as test) sites for the two dates of SAR data were identified separately. Then, using the identified 15 training sites for each of the 3 categories (a total of 45 sites for each date), we developed supervised classification rules on a pixel-by-pixel basis. On the 3 November 1994 SAR image, if a pixel's backscatter is

- \leq -13.60 (*dB*), it is classified as open water,
- > -13.60 *dB* but <-5.68 *dB*, it is classified as non-flooded area, and
- 2 5.68 dB, it is classified as flooded forest.

 On 10 June 1995 SAR data, if a pixel's backscattering coefficient is
- \leq -12.30 dB, it is classified as open water,
- > -12.30 *dB* but <-5.24 *dB*, it is classified as non-flooded area, and
- > -5.24 dB, it is classified as flooded forest.

Next, the classification rules were applied to the original, median-filtered, and adaptive-filtered SAR data of 1994 and 1995 to create inundation maps. Then, the maps were compared non-spatially using descriptive statistics of each classified category, and spatially on a pixel-by-pixel basis. The spatial

comparison created a new layer based on the pixel-by-pixel agreement or disagreement of the two classified images. Table 1 shows all 9 possible outcomes of the agreement and disagreement of the comparison. For instance, if the same pixel (location) on both inundation maps was classified as water, a zero was recoded for that location on the output layer. The 0s, 4s, and 8s represent the agreement and the other values represent the disagreement. Thus, the ratio of the sum (of the 0s, 4s, and 8s) to the total number indicates the degree of agreement. It should be noted that three classified images are created and three comparisons are done at each date. Finally, the accuracy of the inundation maps is assessed using the selected test sites. Figure 3 is the flowchart of the analyses.

Results

Figure 4 shows three classified images or inundation maps using the SAR data on 3 November 1994. Non-flooded areas are represented by white, the flooded forest areas by grey, and open water areas and flat surfaces by black. The map derived from the original SAR data is characterized by many scattered dots and blocks, which is the result of the speckles in the data. The river channel can barely be recognized (Figure 4a). The map derived from the median-filtered SAR data shows some visual improvement having less scattered dots and blocks, and the river channel and surrounding flooded forest are some noticeable (Figure 4b c.f. 4a). The classified image after the adaptive-filtered SAR data has much less scattered dots and blocks, and the river channel and surrounding flooded forests are somewhat clearly delineated (Figure 4c). Similar observations for the inundation maps using the original, median-filtered, and adaptive-filtered SAR data on 10 June 1995 are evident. In summary, the adaptively filtered SAR data has the most visual improvement on the classified images, and may have reduced the speckles and at the same time retain the boundaries.

Table 2 summarizes the areas covered by each category on both dates and clearly demonstrates differences among the extent of each. For instance, on 3 November 1994, the water area covered 23.9%, 21.15%, and 33.2% of the study area as derived from original, median-filtered, and adaptive-filtered SAR

Table 1. On an output layer created by a spatial comparison of two inundation maps on one date, numbers 0 to 8 are used to recode the possible outcomes of the comparison on a pixel-by-pixel basis.

		Inundation Map A		
		Water	Flooded Forest	Nonfloo- ded Area
Inundation Map B	Water	0	1	2
	Flooded Forest	3	4	5
	Nonfloo- ded Area	6	7	8

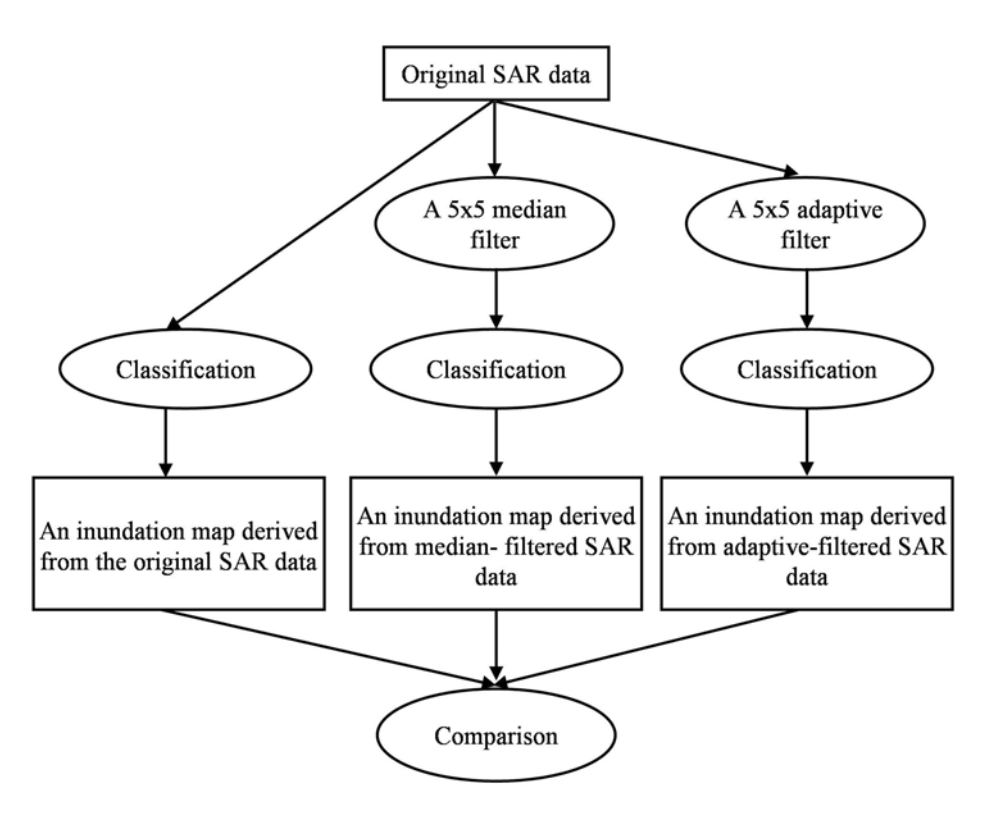


Figure 3. Flowchart of the analysis.

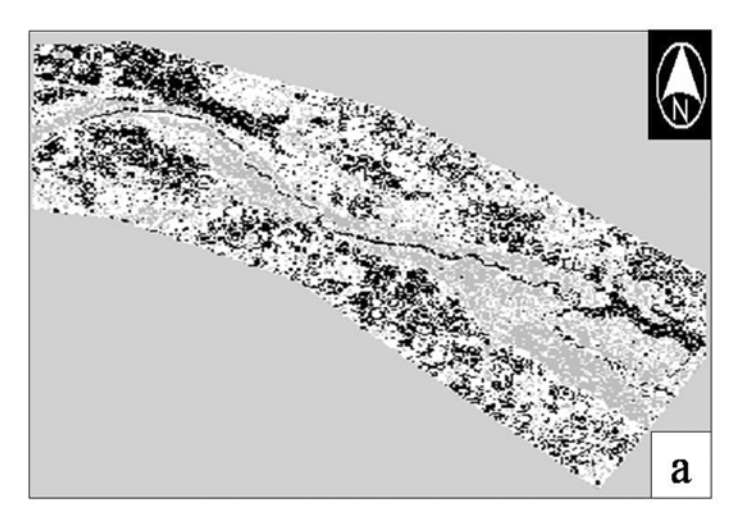
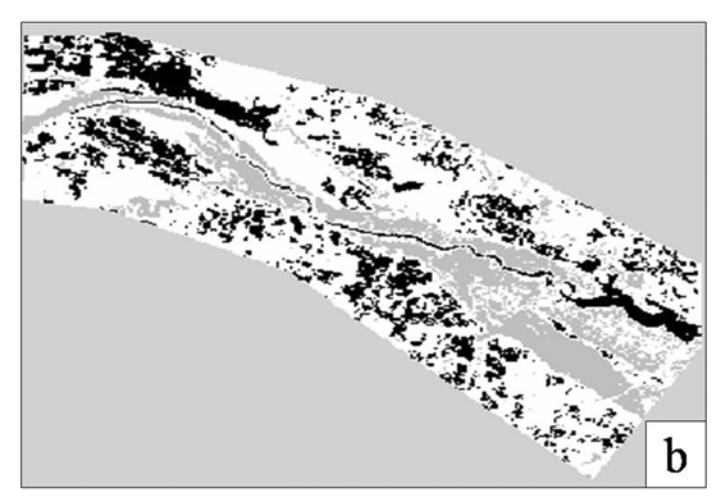
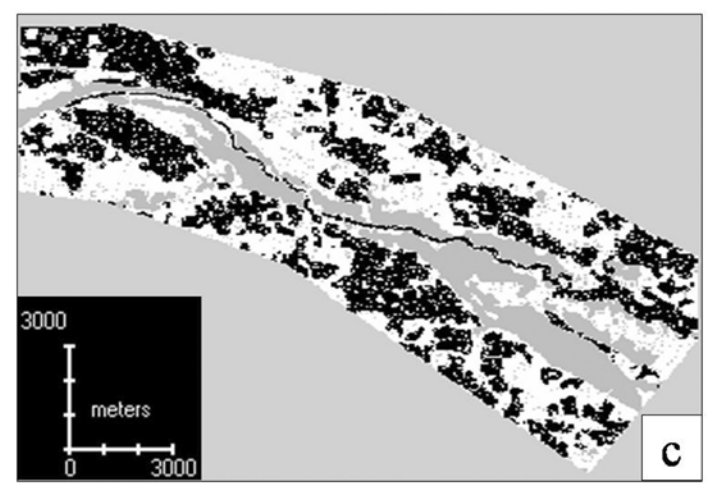


Figure 4. The inundation maps derived from the original (a), median-filtered (b), and adaptive-filtered (c) SAR data of 11/3/1994. Water is shown in black, flooded forest in gray and nonflooded area in white.





data. Because the same classification algorithms were used, the differences are the result of different filtering techniques.

Spatial comparison layers of the three inundation maps derived from 3 November 1994 and 10 June 1995 SAR data were then created. The degree of spatial agreements between the classified images derived from the original data and medianfiltered or the original data and adaptive-filtered data is slightly lower than the degree of spatial agreement of the two classified images derived from the filtered data. Detailed percentages of the agreement or disagreement among the classified images on the two dates are summarized in Table 3. The spatial comparison of the classified images shows that the adaptive-filtered as well as median-filtered SAR data may reduce the speckles, and could also preserve the edges. Figure 5 shows, as an example, the spatial comparison of the inundation maps derived from the median-filtered and adaptive-filtered SAR data acquired on 3 November 1994 (the other spatial correlation layers are similar to this). The agreement and disagreement scattered widely; pixels classified as the same category by both classified images are in white, otherwise in black.

Finally, using 75 test sites (25 test sites for each category) visually identified on the USGS DOQQs, the classification accuracy was evaluated. Due to the temporal change of the inundation extents, test sites on 3 November 1994 and 10 June 1995 were selected independently. Table 4 summarizes the results and four findings are evident. First, the producer's accuracy and user's accuracy (Jensen 1996) derived from the adaptive-filtered or median-filtered SAR data are higher than that derived from the original SAR data for each category. Second, the accuracy derived from the adaptive-filtered or median-filtered SAR data increases or decreases for water or nonflooded category on both dates. Third, the adaptive-filtered SAR data has higher classification accuracy than the median-filtered SAR data do on both dates. Fourth, the adaptive-filtered SAR data has the highest overall classification accuracy. Thus, the adaptive-filter may be better than the median filter in reducing SAR speckles and retaining edges.

Conclusion

An adaptive-filtering method has been developed, which utilized the counts of the pixels of three categories within a moving kernel in order to

Table 2. Statistic summaries of each category from the inundation maps derived from the original, median filtered, and adaptive-filtered SAR data. The area is in km². The percentage of each category of the total study area is in brackets.

11/3/94 Categories		Original	Median-Filtered	Adaptive-Filtered	
Water		30.56 [23.9%]	26.99 [21.1%]	42.56 [33.2%]	
I	Nonflooded Area	70.37 [55.0%]	79.90 [62.4%]	59.65 [46.6%]	
	Flooded Forest	27.07 [21.1%]	21.11 [16.5%]	25.79 [20.2%]	
06/10/95 Categories		Original	Median-Filtered	Adaptive-Filtered	
	Water	25.30 [19.8%]	18.70 [14.6%]	23.58 [18.4%]	
1	Nonflooded Area	65.79 [51.4%]	79.96 [62.5%]	70.63 [55.2%]	
	Flooded Forest	36.88 [28.9%]	29.30 [22.9%]	33.76 [26.4%]	

Table 3. Summary of the spatial agreement among classified images derived from the original, median filtered, and adaptive-filtered SAR data on 3 November 1994 and 10 June 1995.

		% in same (different) category
11/3/1994	Original vs. adaptive-filtered	72.36 (27.64)
	Original vs. median-filtered	72.56 (27.44)
	Median-filtered vs. adaptive-filtered	74.68 (25.32)
6/10/1995	Original vs. adaptive-filtered	66.50 (33.50)
	Original vs. median-filtered	65.98 (34.02)
	Median-filtered vs. adaptive-filtered	77.38 (22.62)

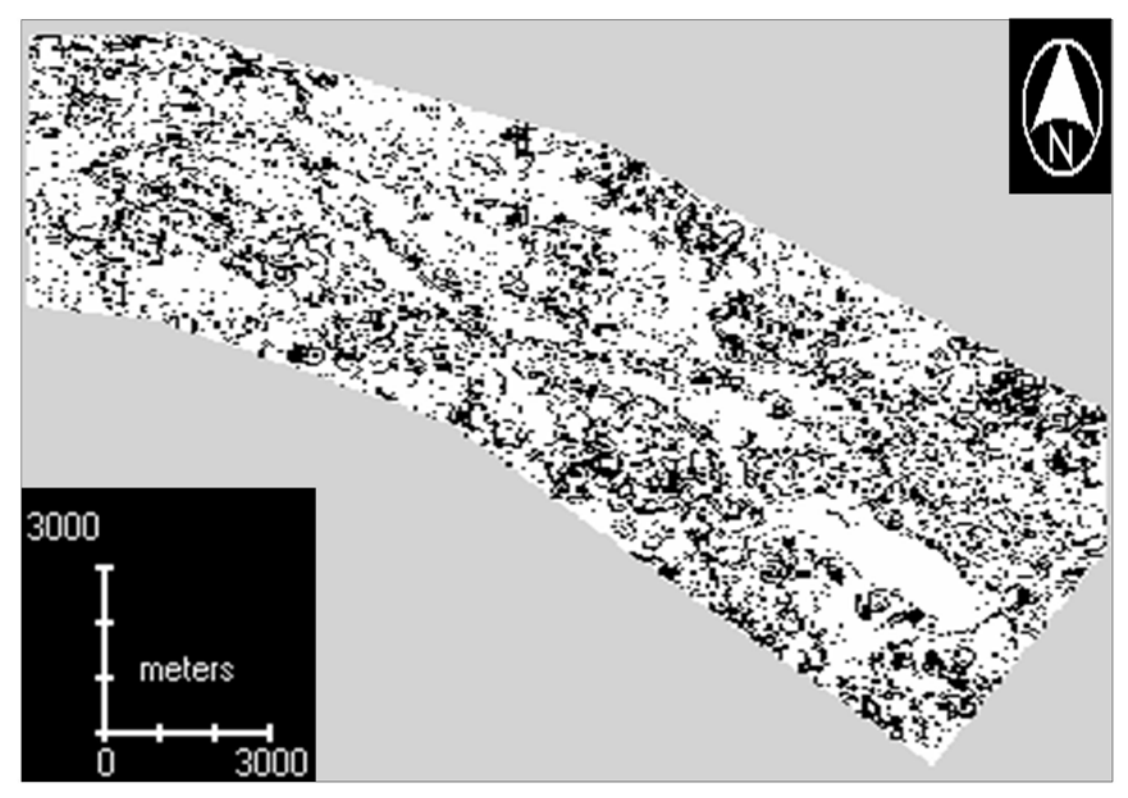


Figure 5. The spatial correlation between the inundation maps derived from the median-filtered and adaptive-filtered SAR data on 3 November 1994. Pixels classified as same category on both maps are in white, otherwise, in black.

Table 4. Error matrix and classification accuracy derived from the original, median-filtered and adaptive-filtered SAR data on both dates.

(a) 3 November 1994. Overall accuracy, 62.5% (original), 70.0% (median-filtered), 74.5% (adaptive-filtered).

		Producer's accuracy (%)	User's accuracy (%)
Original	Open Water	74.6	75.3
	Non-flooded Area	63.2	53.1
	Flooded Forest	53.5	67.4
Median-Filtered	Open Water	82.7	80.8
	Non-flooded Area	74.4	60.2
	Flooded Forest	56.6	78.6
Adaptive-filtered	Open Water	87.9	75.9
	Non-flooded Area	69.1	67.8
	Flooded Forest	71.5	81.9

(b) 10 June 1995. Overall accuracy, 60.7% (original), 72.3% (median-filtered) 78.2% (adaptive-filtered).

		Producer's accuracy (%)	User's accuracy (%)
Original	Open Water	72.6	70.4
	Non-flooded Area	59.1	53.6
	Flooded Forest	54.4	62.8
Median-Filtered	Open Water	81.8	84.8
	Non-flooded Area	75.3	62.7
	Flooded Forest	62.0	62.4
Adaptive-filtered	Open Water	86.7	74.3
	Non-flooded Area	71.2	65.0
	Flooded Forest	75.5	86.3

reduce SAR data speckles and to retain the boundaries. It has been applied to classify two dates of JERS-1 SAR data into water, nonflooded area, and flooded forest categories for a part of the Tar/Pamlico River floodplain of North Carolina. The SAR data were acquired on 3 November 1994 and 10 June 1995. Comparisons of the inundation maps derived from the original, median-filtered, and adaptive-filtered SAR data showed that the adaptive-filtering method reduced the speckles and preserved the boundaries better than the median filter. In addition, the adaptivefiltered SAR data had the highest overall classification accuracy among the median-filtered and non-filtered SAR data. Despite the success of the adaptive filter, there are cautions. First, the adaptive filter depends on pre-defined classification rules that are derived from the training sites on the SAR data after a 5x5 median filtering. The error in the pre-defined classification rules could introduce error in the adaptive filtering method. The adaptive filter based on the original data without pre-defined classification rules should be of advantages, but might difficult to developed due to the wide range of pixel values (backscattering coefficients) within a moving kernel. Second, the adaptive filter determines the filter window's situation only by counting the total number of pixels in each category whereas the spatial distribution within the filter window may provide useful information for adjusting the filtering algorithm. The information could improve the filter's ability to reduce speckles and preserve boundaries.

References

Bourgeau-Chavez, L. L., Kasischke, E. S., Brunzell, S. M., Mudd, J. P. and Smith, K. B. 2001. Analysis of space-borne SAR data for wetland mapping in Virginia riparian ecosystems. *International Journal of Remote Sensing*, 22:3665-3687.

- Hess, L. L., Meleck, J. M., Filoso, S., and Wang, Y. 1995. Delineation of inundated area and vegetation along the Amazon floodplain with the SIR-C synthetic aperture radar. *IEEE Transactions on Geoscience and Remote Sensing*, 33: 896-904.
- Imhoff, M. L., Vermillon, C., Story, M. H., Choudhury, A. M., and Gafoor, A. 1987. Monsoon flood boundary delineation and damage assessment using space borne imaging radar and Landsat data. *Photogrammetric Engineering and Remote Sensing*, 4:405-413.
- Jensen, J. R. 1996. Introductory digital image processing: a remote sensing perspective. 2nd Ed. Prentice Hall, New Jersey.
- Jensen, J. R. 2000. Remote Sensing of the Environment: an Earth Resource Perspective. Prentice Hall, Upper Saddle River, NJ.
- Lee, J. S. 1981. Speckle analysis and smoothing of SAR images. *Journal of Computer Graphics and Image Processing*, 17, 14-32.
- Lee, J. S., Grunes, M. R., and Mango, S. 1991. Speckle reduction in multi-polarization and multi-frequency SAR imagery. *IEEE Transactions on GeoScience and Remote Sensing*, 29 (4), 535-544.
- Lee, J. S., Jurkevich, I., Dewale, P., Wambacq, P., and Oosterlinck, A. 1994. Speckle filtering of synthetic aperture radar images: a review. *Remote Sensing Reviews*, 8, 313-340.
- Lee, J. S., Grunes, M. R., and DeGrandi, G. 1997. Polarimetric SAR speckle filtering and its impact on classification. *The Proceedings of IGARSS'97*. Singapore, August.
- Melack, J. M. and Wang, Y. 1998. Delineation of flooded area and flooded vegetation in Balbina Reservoir (Amazonas, Brazil) with synthetic aperture radar. *Verhandlungen Internationale Vereinigung fur Limnologie*, 26:2374-2377.
- Richards, J. A., Woodgate, P. W., and Skidmore, A. K. 1987. An explanation of enhanced radar backscattering from flooded forests. *International Journal of Remote Sensing*, 8:1093-1100.

Ulaby, F. T., Moore, R. K. and Fung, A. K. 1982. Microwave Remote Sensing: Active and Passive, Vol. II — Radar Remote Sensing and Surface Scattering and Emission Theory. Addison-Wesley, Advanced Book Program, Reading, Massachusetts.

Wang, Y. 2003. Seasonal changes of inundation extent on floodplains detected by JERS-1 SAR data. *International Journal of Remote Sensing*, 21 p. In press.